Depth profile reconstruction of YCrO3 / CaMnO3 superlattices by near total reflection HAXPES

Léo Cambou, Jin-Hong H Lee, Manuel Bibes, Alexandre Gloter, Jean-Pascal Rueff

Depth profile reconstruction of $YCrO_3$ / $CaMnO_3$ superlattices by near total reflection HAXPES

L. Cambou[1], J. H. Lee[2], M. Bibes[2], A. Gloter[3], and J.-P. Rueff [1,4,a)]

[1]Synchrotron SOLEIL, L'Orme des Merisiers, BP 48 St Aubin, 91192 Gif sur Yvette, France
[2]Unité Mixte de Physique CNRS, Thales, Université Paris-Saclay, 91767 Palaiseau, France
[3]Laboratoire de Physique des Solides, CNRS UMR 8502, Université Paris Saclay, 91405 Orsay, France
[4]Laboratoire de Chimie Physique-Matière et Rayonnement, LCPMR, Sorbonne Université, CNRS, Paris F-75005, France
[a)] Electronic mail: jean-pascal.rueff@synchrotron-soleil.fr

We have determined the depth profile of $YCrO_3$ / $CaMnO_3$ superlattices by HAXPES in near total reflection conditions. $YCrO_3$ / $CaMnO_3$ is prone to exhibit interesting magnetotransport properties owing to the large amount of electron transfer expected between Cr^{3+} and Mn^{4+}. The depth profile was reconstructed by simulation of the rocking curves of the different core levels using the YXRO software and fine tuning of the structural model. The results are globally conformed to scanning transmission electron microscopy and electron energy loss spectroscopy analysis except for the top layer whose structure and stoichiometry are found to be preserved in contrast to microscopy.

I. INTRODUCTION

In 2011, SOLEIL Synchrotron along with CEA Saclay and LPS Orsay was awarded a special grant from the LabEx PALM funding agency to invite Prof. C. S. Fadley as a senior chair. The project entitled APTCOM (Advanced Photoemission Techniques for Complex Materials) marked the beginning of the very fruitful and successful collaboration with Chuck Fadley which continues today through different forms. The aim of the APTCOM project was to develop novel synchrotron techniques at SOLEIL synchrotron for detailed characterization of materials including oxide

heterostructures specially at the GALAXIES and CASSIOPEE beamlines which host photoemission endstations. Thanks to C. Fadley's decisive impulse, unique expertise and overall commitment, the outcome of the project turned remarkable leading to numerous publications[1-6] and setting novel approaches at SOLEIL Synchrotron which are still currently used by the scientific community.

During his extraordinarily diverse and rich career, C. Fadley has been continuously promoting the use of hard x-ray photoemission spectroscopy (HAXPES) for investigating complex materials. A specially interesting application of HAXPES is when combined with standing wave approach, thus providing depth sensitive, chemically specific information with atomic resolution as demonstrated in former works by C. Fadley and co-workers. In this article, we illustrate the collaborating work with C. Fadley in a related field with a focus on $YCrO_3$ / $CaMnO_3$ (YCO / CMO) superlattices by HAXPES at near total reflection conditions.

By referring to Zhong et al.[7] density functional theory (DFT) calculations, a perovskite oxide interface between Cr^{3+} and Mn^{4+} system may give rise to a large amount of electron transfer from Cr^{3+} to Mn^{4+} since the difference between their Fermi energies after aligning their oxygen states is large (~2 eV). We have chosen two antiferromagnetic insulators, *i.e.* YCO and CMO, in consideration of possible interfacial doping in the CMO layer. It is known that CMO shows a metallic behavior around room temperature by doping 1-2% of electrons in the system[8]. In addition, interesting magnetotransport phenomena at the interface such as topological Hall effect[9] may appear. Finally, and as detailed below, YCO and CMO can both be grown by pulsed laser deposition (PLD) at high oxygen pressure. This does not apply to other perovskite material pairs prone to

charge transfer such as those including rare-earth titanates or vanadates which require low pressure to stabilize Ti^{3+} and V^{3+} ions, and are often combined with nickelates, cobaltates or manganites, grown at high pressure. In such cases, oxygen vacancies or interstitials / antisites may be present in the structure, hampering an interpretation of the properties of the heterostructures in terms of charge transfer only[10,11].

II. EXPERIMENTAL

A. Sample growth

The YCO / CMO superlattice was grown on a $NdAlO_3$ (001) (NAO) substrate by pulsed laser deposition (PLD). The superlattice sample consists of five periods where one period corresponds to 5 unit cells (uc) of YCO and 5 uc of CMO. The growth temperature for YCO was 750°C and for CMO it was 650°C. During the growth, the oxygen pressure was fixed to 0.2 mbar and the KrF excimer laser was used in order to ablate the stoichiometric target of YCO and CMO by the fluence of ~2 J cm^{-2} and repetition rate of 5 Hz. After the growth, the sample was *in-situ* post-annealed at 500°C for 30 minutes in ~500 mbar of oxygen.

The structure of the superlattice sample is schematized in Figure 1a. It consists of 5 repetitions of a CMO / YCO bilayer, deposited on a NAO substrate. Both CMO and YCO layer are composed of 5 uc. The d-spacing of the superlattice is 37.7 Å.

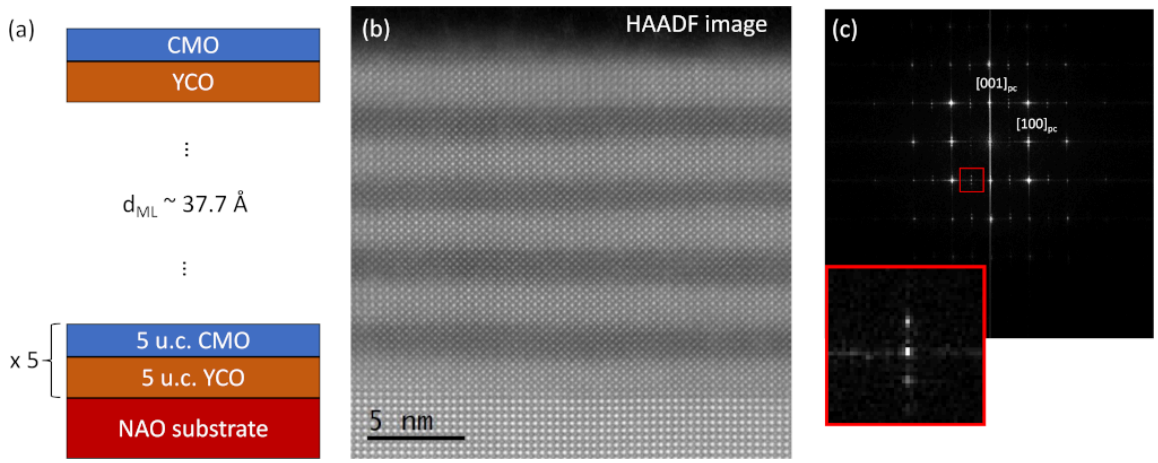

FIG. 1. (a) schematized structure of the CMO / YCO superlattice; (b) HAADF-STEM image; (c) diffractogram of the HAADF-STEM image of the substrate and the superlattice showing a cube of coherent growth. The super-periodicity, enlarged in the inset, is measured at 38 Å.

The sample crystalline quality was verified by high resolution High-Angle Annular Dark-Field - Scanning Transmission Electron Microscopy (HAADF-STEM) at LPS using the Nion STEM microscope operated at 100keV. The HAADF image and its diffractogram shown in Figure 1b,c attest of the coherent growth of the superlattice with the NAO substrate. The CMO and YCO layers are clearly visible in the HAADF contrast (due to the heavier Y atom), showing a perfect crystallinity except for the top CMO layer.

B. HAXPES measurements

The depth profile was further characterized by HAXPES near total reflection conditions. The measurements were carried out at the GALAXIES undulator beamline at SOLEIL Synchrotron on the HAXPES endstation. Details of the beamline has been described elsewhere[12]. The sample was mounted on an omicron plate with carbon tape and installed onto the HAXPES 4-axes manipulator. The beamline energy was selected

by a double crystal Si(111) cryogenically cooled monochromator. All HAXPES spectra were acquired at room temperature.

The Y, Mn, O, Ca, Cr, core-level spectra were measured as a function of the incident angle at a photon energy of 3000 eV. The results are summarized in Figure 2.

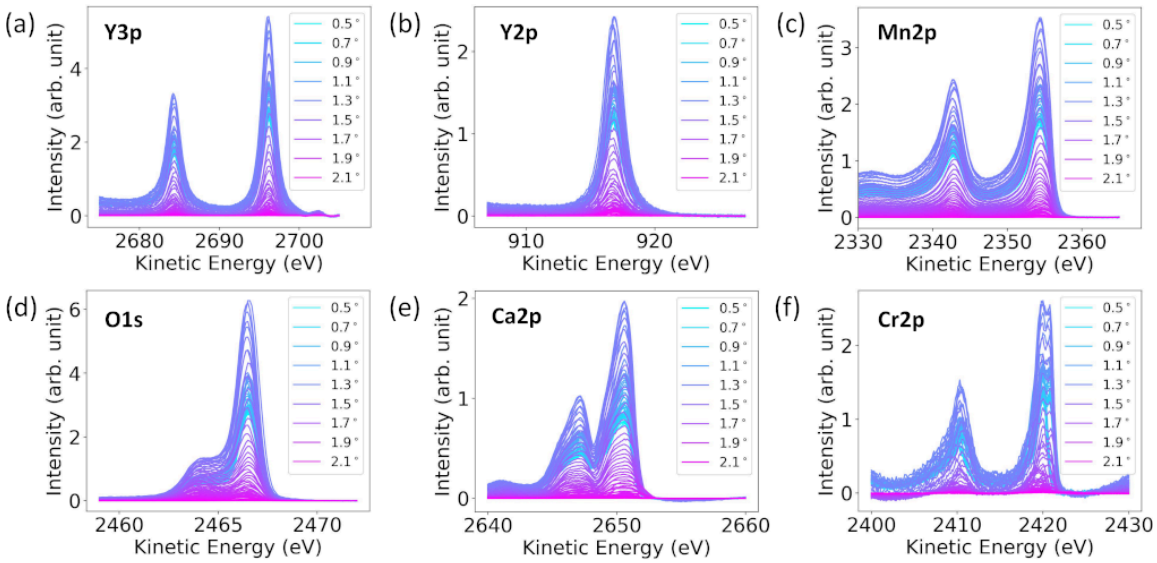

FIG. 2. Angular dependence of the HAXPES spectra for Y3p (a), Y2p (b), Mn2p (c), O1s (d), Ca2p (e), Cr2p (f) core-levels in YCO / CMO superlattice.

The spectra exhibit a strong variation intensity depending on the incident angle when approaching the total reflection conditions. The resulting rocking curves are represented with open circles in Figure 5b for the different core levels Mn2p, Cr2p, Ca2p, O1s and Y3p; Y2p was disregarded as it follows closely the behavior of Y3p. They were extracted from the HAXPES data by integrating the intensity under the curve after removal of a Shirley background. No other normalization of the data was performed as the beam intensity is nearly constant at fixed photon energy. The position of the rocking curve maxima provides a first view of the in-depth structure: Cr2p and Y3p rocking curves appear shifted towards higher angles with respect to Mn2p and Ca2p in agreement

with structure of the first layers consisting of CMO on YCO. The analysis of the rocking curve will be discussed in more details in section III.

C. STEM – EELS

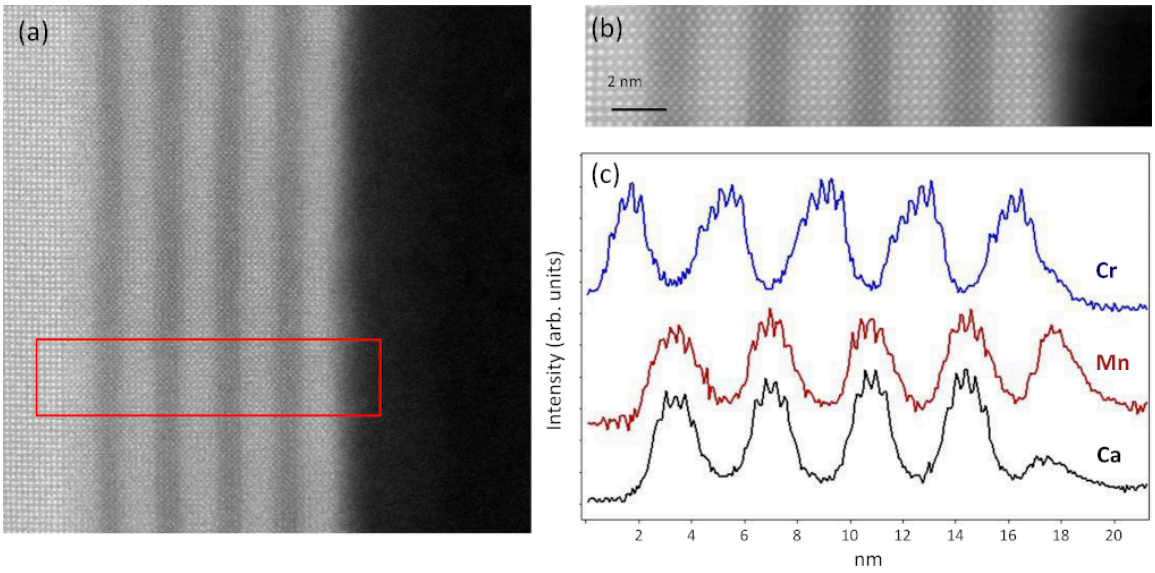

FIG. 3 (a) HAADF-STEM image, the red box indicates the area for STEM-EELS spectromicroscopy; (b) HAADF-STEM obtained during the STEM-EELS measurement, (c) Cr, Mn, Ca profiles obtained from the Cr2p, Mn2p and Ca2p EELS edges.

The sample cross-sections for STEM-EELS measurements were prepared by FIB in several steps. A series of protective layers were first deposited using *ex-situ* carbon deposition by thermal evaporation (ca. 50 nm), *in-situ* Pt deposition by e-beam (ca. 200 nm) and, *in-situ* Pt deposition by Ga-beam (ca. 1500 nm). A thick lamella was then extracted with a 30 keV Ga beam to obtain an electron transparent lamella using 30 keV to 2 keV Ga beams successively. We used typical beam currents to achieve a full sample lamella preparation of ca. 15 (length) x10 (depth) µm in ca. 4 hours. While such procedure normally yields undamaged lamellae, the EELS results in Figure 3 show that the topmost CMO layer is severely Ca-depleted while no strong change is found in the Mn stoichiometry. Furthermore, we observe that the top CMO layers have different Mn^{3+}

content as a function of the local thicknesses confirming probable damages during the sample preparation. Carbon was also detected by EELS at the last nanometer of the CMO top layer. This further indicates that some of the protective carbon layer deposited before the FIB sample thinning is intermixed or overlapped with the top oxide layer, suggesting some damage or artefact has been done during the sample preparation for STEM. Such FIB damages were already reported in materials down to several nm in depth [13,14]. Insulating samples are especially prone to damages due to the effects of charging or deflected beam[15]. The *ex-situ* carbon deposition can reduce the overall charging but it might have been insufficient here due to the very insulating nature of the NAO substrate.

III. Rocking curve Analysis and Discussion

A. Global reconstruction

To reconstruct the depth profile of the superlattice, we carried out simulation of the angular dependence of the photoemission yield using the YXRO code[16]. The code takes a structural model of the layers stacking as input and computes the angular dependence of the photoemission yield for the different elements present in the materials. By tuning the model parameters (layers composition, density, thickness, interdiffusion) to fit the experimental rocking curves, it is then possible to reconstruct the stacking depth profile with atomic resolution.

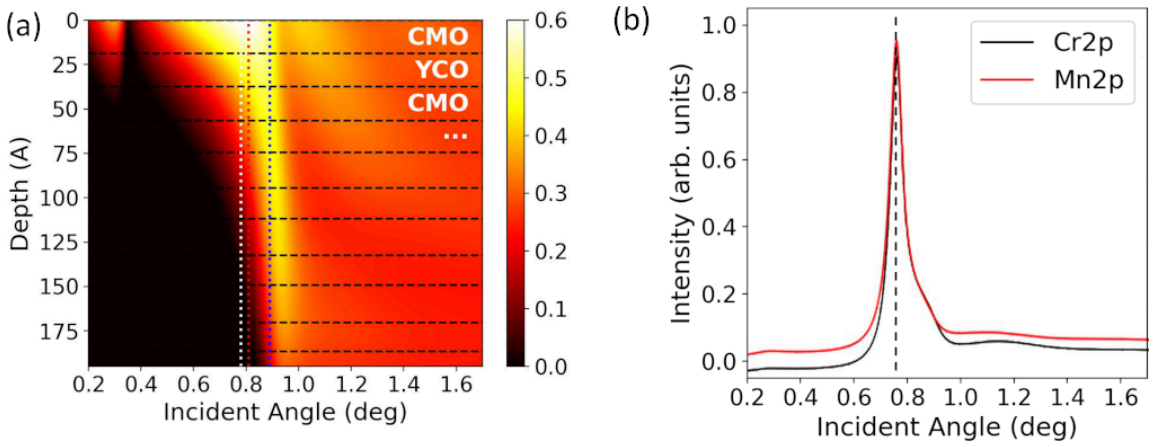

FIG. 4. (a) YXRO computed electric field strength distribution in YCO / CMO as a function of the depth and incident angle; (b) depth integrated photoemission yield for Cr and Mn 2p. The dashed lines are discussed in the text.

Figure 4 displays results of the YXRO simulations in the YCO / CMO superlattice. The intensity map in Figure 4a represents the distribution of the electric field strength as a function of depth and incident angle. The intense area near 0.8° marks the total reflection region (white dashed line in Figure 4a). The total reflection peak appears more clearly in Figure 4b (black dashed line) showing the depth integrated photoemission yield for Cr2p and Mn2p. Because of the limited number of repetitions of the superlattice, there is no marked Bragg like standing wave modulation. A weak modulation can be observed around 1.2° and ~1.7° corresponding to the superlattice Bragg peaks but this cannot be exploited because of its low intensity.

Figure 5b shows the calculated rocking curve for the best structural model schematized in Figure 5a. The simulations fit well the experimental rocking curves of all considered core levels. The structural model is found to resemble closely the initial structure except for the addition of an extra layer on top, likely due C contamination with 10 Å interdiffusion. In contrast to the STEM image, we found that the top CMO layer

remains well defined without interdiffusion or change in stoichiometry. A change of the CMO top layer composition in the simulation leads to a poorer fit of the Ca rocking curve (dashed line in Figure 5b). We believe the sample used for STEM – EELS may have been damaged during the FIB process, explaining the difference with the HAXPES results.

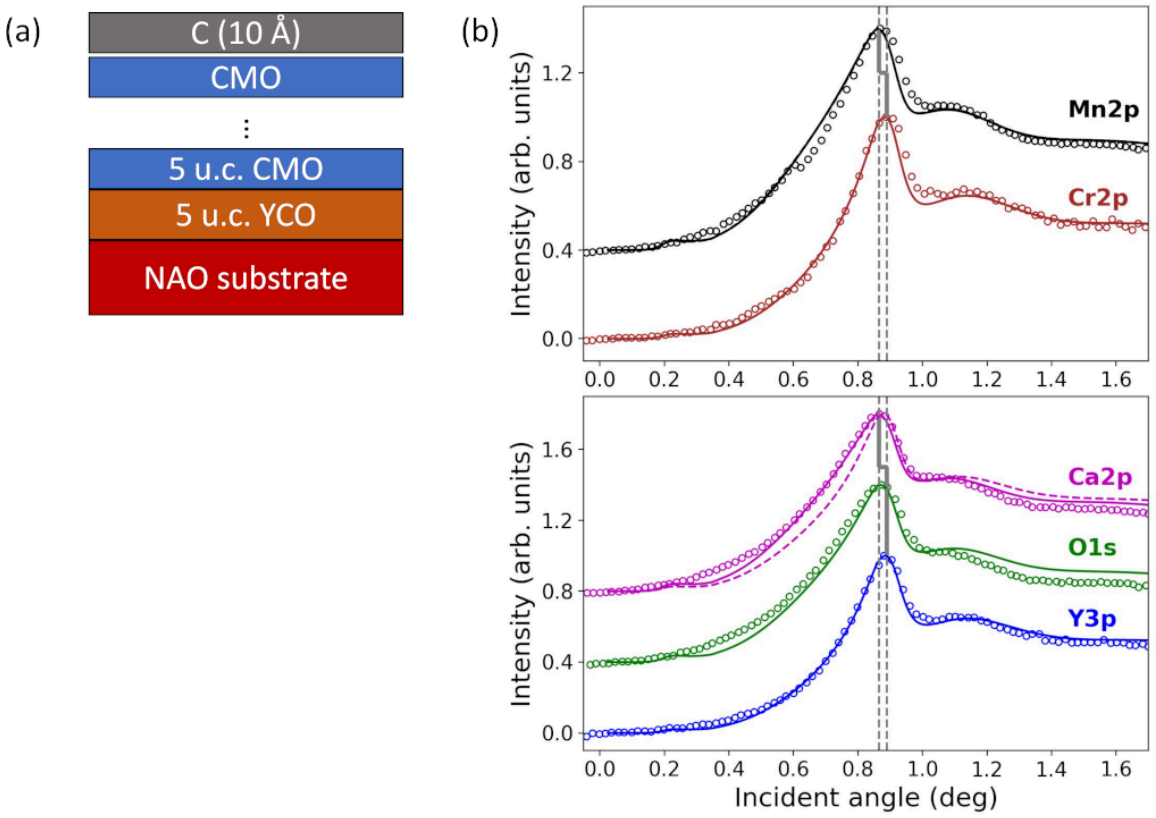

FIG. 5. (a) Optimized structural model; (b) experimental (open circles) and simulated rocking curves for the different core levels using the optimized model (solid lines) and for the damaged structure with a Ca depleted surface layer (dashed line).

B. Surface components analysis

The O and Ca spectra can be further decomposed into two sub-components of low binding energy (LBE) and high binding energy (HBE) due to different chemical environment as presented in Figures 6a,c ; the respective rocking curves are shown in Figures 6b,d. The O1s LBE rocking curve is shifted towards higher angles with respect to

HBE with a maximum at 0.88° against 0.82° for HBE. According to the electric field map in Figure 4a, the LBE thus probes deep inside the whole structure (see the blue dashed line in Figure 4a) whereas the HBE comes from the ~3 surface layers (red dashed line in Figure 4a).

Similarly, the LBE peak in Ca is reminiscent of bulk Ca whereas the HBE peak is related to the surface layers. We carried out simulations of the LBE and HBE rocking curves of the O1s and Ca2p core-level by assuming that the top CMO only take part in the HBE signal. The simulated rocking curves (lines in Figure 6b,d) fit reasonably well the experimental data, especially the HBE one. The simulated LBE rocking curve shows differences but the position of the rocking curve is well reproduced. This analysis further confirms the CMO is properly crystallized on top without stoichiometric changes. Finally, based on our previous work in BFO / CCMO[1], we can tentatively assign the HBE component to the presence of oxygen vacancies in the topmost CMO layer(s).

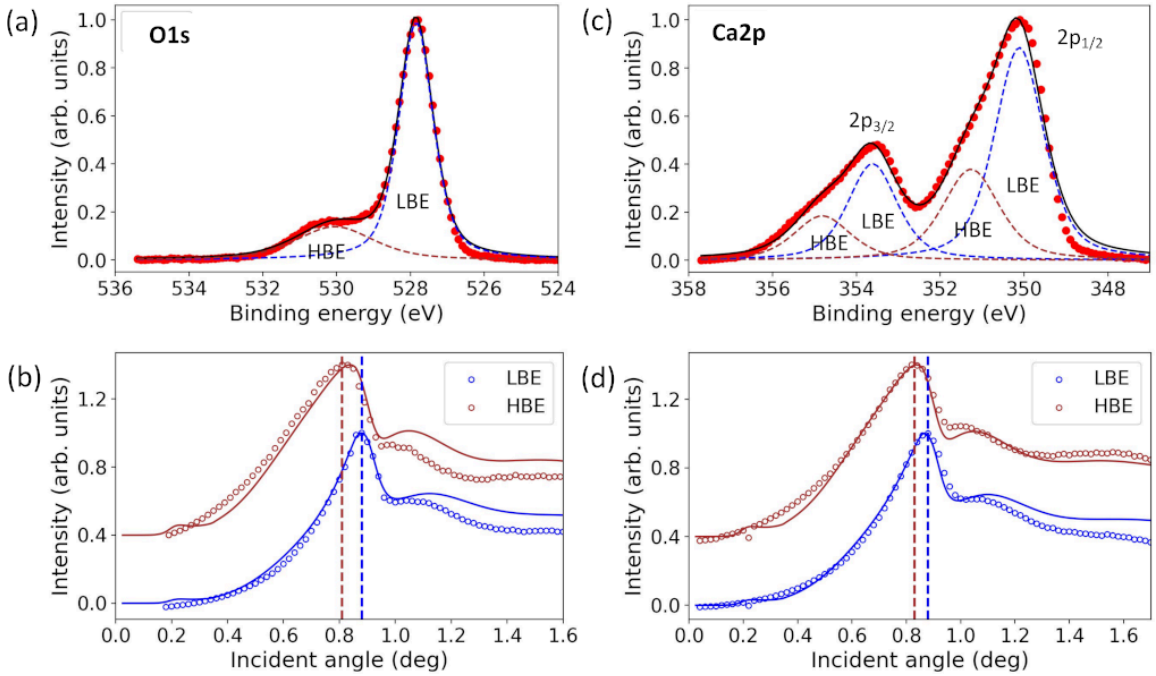

FIG. 6. Decomposition of O1s (a) and Ca2p (b) photoemission spectrum in low binding energy (LBE) and high binding energy (HBE) components and resulting rocking curves for O (b) and Ca 2p3/2 (d) respectively.

IV. SUMMARY AND CONCLUSIONS

In summary, we have investigated the in-depth electronic properties of YCO / CMO layers by HAXPES in near total reflection conditions. The simulations of the rocking curves for the different elements confirm the samples crystalline quality with unchanged stoichiometry including the top layers, somewhat contrasting with the STEM – EELS data.

ACKNOWLEDGMENTS

This work is supported by two public grants overseen by the French National Research Agency (ANR) as part of the "Investissements d'Avenir" program: Labex NanoSaclay, reference: ANR-10-LABX-0035, and the LabEx PALM, reference: ANR-10-LABX-0039. We acknowledge SOLEIL Synchrotron for provision of beamtime. We warmly thank S. Nemsak for advice on improving the data analysis and simulations using YXRO software. Finally, we are indebted to C. Fadley for his incentive of combining HAXPES with standing waves at the GALAXIES beamline, and continuous support to our work.

DATA AVAILABILITY

Raw data were generated at the Synchrotron SOLEIL large scale facility. Derived data supporting the findings of this study are available from the corresponding author upon reasonable request.

REFERENCES

[1]M. Marinova, J. E. Rault, A. Gloter, S. Nemsak, G. K. Palsson, J.-P. Rueff, C. S. Fadley, C. Carrétéro, H. Yamada, K. March, V. Garcia, S. Fusil, A. Barthélémy, O. Stéphan, C. Colliex, and Manuel Bibes, Nano Letters **15**, 2533 (2015).

[2]M. N. Grisolia, J. Varignon, G. Sanchez-Santolino, A. Arora, S. Valencia, M. Varela, R. Abrudan, E. Weschke, E. Schierle, J. E. Rault, J. P. Rueff, A. Barthélémy, J. Santamaria, and M. Bibes, Nature Physics **12**, 484 (2016).

[3]S.-C. Lin, C.-T. Kuo, R. B. Comes, J. E. Rault, J.-P. Rueff, S. Nemsak, A. Taleb, J. B. Kortright, J. Meyer-Ilse, E. Gullikson, P. V. Sushko, S. R. Spurgeon, M. Gehlmann, M. E. Bowden, L. Plucinski, S. A. Chambers, and C. S. Fadley, Interface properties and built-in potential profile of a $LaCro_3/SrTio_3$ superlattice determined by standing-wave excited photoemission spectroscopy, Phys. Rev. B **98**, 165124 (2018).

[4]G. Conti, S. Nemsak, C.-T. Kuo, M. Gehlmann, C. Conlon, A. Keqi, A. Rattanachata, O. Karslioglu, J. Mueller, J. Sethian, H. Bluhm, J. E. Rault, J.-P. Rueff, H. Fang, A. Javey, and C. S. Fadley, APL Materials **6**, 058101 (2018).

[5]C. S. Conlon, G. Conti, S. Nemsak, G. Palsson, R. Moubah, C. T. Kuo, M. Gehlmann, J. Ciston, J. Rault, J. P. Rueff, F. Salmassi, W. Stolte, A. Rattanachata, S. C. Lin, A. Keqi, A. Saw, B. Hjörvarsson, and C. S. Fadley, Journal of Applied Physics **126**, 075305, (2019).

[6]S.-C. Lin, C.-T. Kuo, Y.-C. Shao, Y.-D. Chuang, J. Geessinck, M. Huijben, J.-P. Rueff, I. L. Graff, G. Conti, Y. Peng, A. Bostwick, E. Rotenberg, E. Gullikson, S. Nemsak, A. Vailionis, N. Gauquelin, J. Verbeeck, G. Ghiringhelli, C. M. Schneider, and C. S. Fadley, Phys. Rev. Materials **4**, 115002 (2020).

[7]Z. Zhong and P. Hansmann, Phys. Rev. X **7**, 011023 (2017).

[8]P.-H. Xiang, H. Yamada, H. Akoh and A. Sawa, J. Appl. Phys. **112**, 113703 (2012).

[9]L. Vistoli, W. Wang, A. Sander, Q. Zhu, B. Casals, R. Cichelero, A. Barthélémy, S. Fusil, G. Herranz, S. Valencia, R. Abrudan, E. Weschke, K. Nakazawa, H.

Kohno, J. Santamaria, W. Wu, V. Garcia and M. Bibes, Nature Physiscs **15**, 67 (2019).

[10]A. S. Disa, D. P. Kumah, A. Malashevich, H. Chen, D. A. Arena, E. D. Specht, S. Ismail-Beigi, F. J. Walker, and Charles H. Ahn, Phys. Rev. Lett. **114**, 026801 (2015).

[11]G. Araizi-Kanoutas, J. Geessinck, N. Gauquelin, S. Smit, X. H. Verbeek, S. K. Mishra, P. Bencok, C. Schlueter, T.-L. Lee, D. Krishnan, J. Fatermans, J. Verbeeck, G. Rijnders, G. Koster, and Mark S. Golden, Phys. Rev. Materials **4**, 026001 (2020).

[12]J.-P. Rueff, J. M. Ablett, D. Céolin, D. Prieur, Th. Moreno, V. Balédent, B. Lassalle, J. E. Rault, M. Simon, and A. Shukla, J. Synchrotron Rad. **22**, 175 (2015).

[13]W. Siemons, C. Beekman, J. D. Fowlkes, N. Balke, J. Z. Tischler, R. Xu, W. Liu, C. M. Gonzales, J. D. Budai and H. M. Christen, APL Materials **2**, 022109 (2014)

[14]J. P. McCaffrey, M. W. Phaneuf, and L. D.Madsen, Ultramicroscopy **87** 97, (2001)

[15]K. Park, C. Yang, K. Kim, D. Nam, K. Hwang, J. Bae, J. Ahn, J. Choi, S. Park, S. Jeong, H. Cho, and E. Jeong, Proceedings of the SPIE, 8819, 88190I (2013)

[16]S.-H. Yang, A. X. Gray, A. M. Kaiser, B. S. Mun, B. C. Sell, J. B. Kortright, and C. S. Fadley, Journal of Applied Physics **113**, 073513 (2013).